

**$\beta$ -delayed two-proton decay of  $^{27}\text{S}$  at the proton-drip line**

G. Z. Shi (石国柱),<sup>1,2,3,\*</sup> J. J. Liu (刘嘉健),<sup>1,\*</sup> Z. Y. Lin (林喆阳),<sup>1,2</sup> H. F. Zhu (朱浩帆),<sup>1,4</sup> X. X. Xu (徐新星),<sup>1,5,6,3,7,†</sup> L. J. Sun (孙立杰),<sup>6,8,‡</sup> P. F. Liang (梁鹏飞),<sup>5</sup> C. J. Lin (林承键),<sup>6,9</sup> J. Lee (李晓菁),<sup>5</sup> C. X. Yuan (袁岑溪),<sup>10</sup> S. M. Wang (王思敏),<sup>11</sup> Z. H. Li (李智焕),<sup>11</sup> H. S. Xu (徐瑚珊),<sup>1,3,7</sup> Z. G. Hu (胡正国),<sup>1,3,7</sup> Y. Y. Yang (杨彦云),<sup>1</sup> R. F. Chen (陈若富),<sup>1</sup> J. S. Wang (王建松),<sup>12,1</sup> D. X. Wang (王东玺),<sup>6</sup> H. Y. Wu (吴鸿毅),<sup>11</sup> K. Wang (王康),<sup>1,13</sup> F. F. Duan (段芳芳),<sup>1,2</sup> Y. H. Lam (蓝乙华),<sup>1,3</sup> P. Ma (马朋),<sup>1</sup> Z. H. Gao (高志浩),<sup>1,2</sup> Q. Hu (胡强),<sup>1</sup> Z. Bai (白真),<sup>1</sup> J. B. Ma (马军兵),<sup>1</sup> J. G. Wang (王建国),<sup>1</sup> F. P. Zhong (钟福鹏),<sup>9,6</sup> C. G. Wu (武晨光),<sup>11</sup> D. W. Luo (罗迪雯),<sup>11</sup> Y. Jiang (蒋颖),<sup>11</sup> Y. Liu (刘洋),<sup>11</sup> D. S. Hou (侯东升),<sup>1,3</sup> R. Li (李忍),<sup>1,3</sup> N. R. Ma (马南茹),<sup>6</sup> W. H. Ma (马维虎),<sup>1,14</sup> G. M. Yu (余功明),<sup>1,15</sup> D. Patel,<sup>1,16</sup> S. Y. Jin (金树亚),<sup>1,3</sup> Y. F. Wang (王煜峰),<sup>1,17</sup> Y. C. Yu (余悦超),<sup>1,17</sup> Q. W. Zhou (周清武),<sup>1,18</sup> P. Wang (王鹏),<sup>1,18</sup> L. Y. Hu (胡力元),<sup>15</sup> X. Wang (王翔),<sup>11</sup> H. L. Zang (臧宏亮),<sup>11</sup> P. J. Li (李朋杰),<sup>5</sup> Q. R. Gao (高祺锐),<sup>1</sup> H. Jian (简豪),<sup>1</sup> S. X. Zha (查思贤),<sup>1,3</sup> F. C. Dai (戴凡超),<sup>1,3</sup> R. Fan (范锐),<sup>1,3</sup> Q. Q. Zhao (赵青青),<sup>5</sup> L. Yang (杨磊),<sup>6</sup> P. W. Wen (温培威),<sup>6</sup> F. Yang (杨峰),<sup>6</sup> H. M. Jia (贾会明),<sup>6</sup> G. L. Zhang (张高龙),<sup>19</sup> M. Pan (潘敏),<sup>19,6</sup> X. Y. Wang (汪小雨),<sup>19</sup> H. H. Sun (孙浩瀚),<sup>6</sup> X. H. Zhou (周小红),<sup>1,3,7</sup> Y. H. Zhang (张玉虎),<sup>1,3,7</sup> M. Wang (王猛),<sup>1,3,7</sup> M. L. Liu (柳敏良),<sup>1</sup> H. J. Ong (王惠仁),<sup>1,3,20,21</sup> and W. Q. Yang (杨维青)<sup>1</sup>

<sup>1</sup>CAS Key Laboratory of High Precision Nuclear Spectroscopy, Institute of Modern Physics, Chinese Academy of Sciences, Lanzhou 730000, China

<sup>2</sup>School of Nuclear Science and Technology, Lanzhou University, Lanzhou 730000, China

<sup>3</sup>School of Nuclear Science and Technology, University of Chinese Academy of Sciences, Beijing 100049, China

<sup>4</sup>School of Physics and Engineering, Zhengzhou University, Zhengzhou 450001, China

<sup>5</sup>Department of Physics, The University of Hong Kong, Hong Kong, China

<sup>6</sup>Department of Nuclear Physics, China Institute of Atomic Energy, Beijing 102413, China

<sup>7</sup>Advanced Energy Science and Technology Guangdong Laboratory, Huizhou 516003, China

<sup>8</sup>School of Physics and Astronomy, Shanghai Jiao Tong University, Shanghai 200240, China

<sup>9</sup>College of Physics and Technology, Guangxi Normal University, Guilin 541004, China

<sup>10</sup>Sino-French Institute of Nuclear Engineering and Technology, Sun Yat-Sen University, Zhuhai 519082, China

<sup>11</sup>State Key Laboratory of Nuclear Physics and Technology, School of Physics, Peking University, Beijing 100871, China

<sup>12</sup>College of Science, Huzhou University, Huzhou 313000, China

<sup>13</sup>Shanghai Institute of Applied Physics, Chinese Academy of Sciences, Shanghai 201800, China

<sup>14</sup>Institute of Modern Physics, Fudan University, Shanghai 200433, China

<sup>15</sup>Fundamental Science on Nuclear Safety and Simulation Technology Laboratory, Harbin Engineering University, Harbin 150001, China

<sup>16</sup>Department of Physics, Sardar Vallabhbhai National Institute of Technology Surat 395007, India

<sup>17</sup>School of Physics and Astronomy, Yunnan University, Kunming 650091, China

<sup>18</sup>School of Physical Science and Technology, Southwest University, Chongqing 400044, China

<sup>19</sup>School of Physics and Nuclear Energy Engineering, Beihang University, Beijing 100191, China

<sup>20</sup>RCNP, Osaka University, Osaka 567-0047, Japan

<sup>21</sup>Joint Department for Nuclear Physics, Lanzhou University and Institute of Modern Physics, CAS, Lanzhou 730000, China



(Received 3 March 2021; accepted 21 May 2021; published 15 June 2021)

The  $\beta$ -delayed two-proton ( $\beta 2p$ ) decay of  $^{27}\text{S}$  was studied using a state-of-the-art silicon array and Clover-type HPGe detectors. An energy peak at 6372(15) keV with a branching ratio of 2.4(5)% in the decay-energy spectrum was identified as a two-proton transition via the isobaric-analog state in  $^{27}\text{P}$  to the ground state of  $^{25}\text{Al}$  in the  $\beta$  decay of  $^{27}\text{S}$ . Two-proton angular correlations were measured by the silicon array to study the mechanism of two-proton emission. Based on experimental results and Monte Carlo simulations, it was found that the main mechanism for the emission of  $\beta 2p$  by  $^{27}\text{S}$  is of sequential nature.

DOI: [10.1103/PhysRevC.103.L061301](https://doi.org/10.1103/PhysRevC.103.L061301)

\*These authors contributed equally to this work and should be considered co-first authors.

<sup>†</sup>xinxing@impcas.ac.cn

<sup>‡</sup>sunli@frib.msu.edu

Nuclei far from the  $\beta$ -stability line exhibit various decay modes [1–3]. Of particular interest are the  $\beta$ -delayed one- or multiparticle emissions, which become more dominant near the neutron or proton drip lines and provide access to the nuclear structure properties. One of the interesting decay modes is the  $\beta$ -delayed two-proton ( $\beta 2p$ ) emission, which is a rare decay process for nuclei in the proton-rich region with the

window of  $Q_{\beta^+} - S_{2p} > 0$ . The exotic phenomenon of  $\beta 2p$  decay was first predicted and discussed by Goldanskii [4]. It was followed almost immediately by the first experiment performed by Cable *et al.* [5], in which two  $2p$  transitions to the first-excited and ground state of  $^{20}\text{Ne}$  were observed in the  $\beta$  decay of  $^{22}\text{Al}$ . A number of  $\beta 2p$  emitters have been identified since then [1–3]. Recently, a  $\beta 2p$  emission through the isobaric-analog state (IAS) of  $^{22}\text{Al}$  was observed in the decay of  $^{22}\text{Si}$ , the lightest nucleus with  $T_z = -3$  in the nuclide chart [6].

In the  $\beta 2p$  emission, energy and momentum conservation [7] are not sufficient to fully explain the momenta and energy distribution between emitted protons. In general, the two-proton emission can be classified as follows: (1) direct emission, where two protons escaping simultaneously show strong correlations, and (2) sequential emission, where two protons emitted through an intermediate state can be treated as two independent protons. Based on branching ratios and decay widths calculated by shell model, it was predicted that only a small percentage of direct emission happened in  $\beta 2p$  [8]. Indeed, all experiments performed thus far have indicated that the predominant mechanism of the emission is sequential. Two individual experiments on the  $\beta$  decay of  $^{22}\text{Al}$  were performed by Cable *et al.* [5] and Wang *et al.* [9], which reported an upper limit of 15% and 29(13)% for the direct emission, respectively. However, both experiments did not have sufficient statistics to draw a conclusion. On the other hand, it has been shown that the detailed analysis of the  $\beta 2p$  mechanism of  $^{31}\text{Ar}$  provides precise data for studying nuclear structure [10,11].

The first decay spectroscopy of  $^{27}\text{S}$  was performed by implanting the ions into silicon detectors [12].  $\beta 2p$  from the IAS at 12 MeV of  $^{27}\text{P}$  to the ground state of  $^{25}\text{Al}$  was observed, but no other decay channel was reported due to the low statistics and high contamination. Cachel *et al.* repeated the experiment by using the similar method and observed several high-energy  $\beta$ -delayed proton branches [13]. The successful determination of absolute branching ratios of two low-energy proton transitions were achieved via a time-projection chamber technique [14]. Recently, the emissions of  $\beta$ -delayed one proton and  $\gamma$  by  $^{27}\text{S}$  were measured by Sun *et al.* [15]. The precise decay data of  $^{27}\text{S}$  gave an experimental constraint on the  $^{26}\text{Si}(p, \gamma)^{27}\text{S}$  reaction rate, confirming that the dominant contribution of the galactic  $^{26}\text{Al}$  synthesis is from the  $\beta^+$  decay of  $^{26}\text{Si}$  [16]. In this Letter, we report on the results of the two-proton emission from the IAS of  $^{27}\text{P}$  to the ground state of  $^{25}\text{Al}$  in the  $\beta$  decay of  $^{27}\text{S}$  and discuss its mechanism based on measured angular correlations.

The  $\beta$ -decay experiment of  $^{27}\text{S}$  was performed at the National Laboratory of Heavy Ion Research Facility of Lanzhou (HIRFL) [17]. The nuclei of interest were produced via the projectile fragmentation of a 80.6 MeV/nucleon  $^{32}\text{S}^{16+}$  primary beam impinging upon a 1581- $\mu\text{m}$ -thick  $^9\text{Be}$  target. The projectile fragments were separated and purified using the Radioactive Ion Beam Line in Lanzhou (RIBLL1) [18]. The ions in the secondary beam were identified by using the energy loss ( $\Delta E$ ) and time-of-flight (ToF) information obtained with two quadrant silicon detectors (QSDs) and two plastic scintillators, respectively. During the 95.3-hour

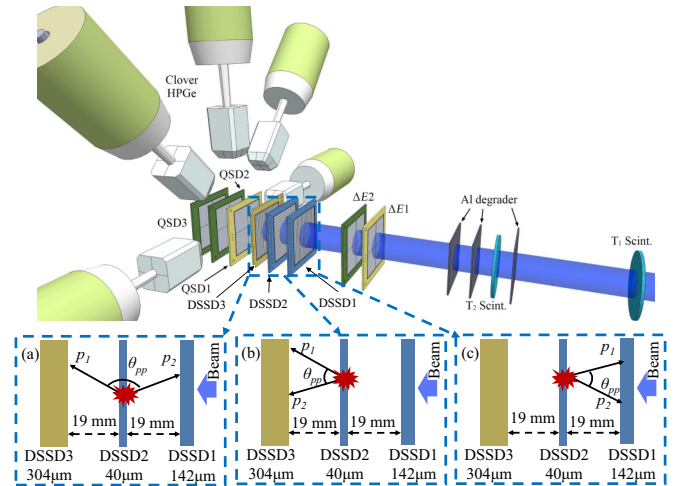


FIG. 1. Schematic layout of the detection system locating at Terminal 2 of the RIBLL1. The zoom-in figures for silicon array marked with (a), (b), and (c) demonstrate the methods for the proton-proton coincidence. The  $^{27}\text{S}$  ions were stopped by DSSD2 and the escaping two protons after  $\beta$  decay,  $p_1$  and  $p_2$ , were (a) separately measured by DSSD3 and DSSD1, both measured by (b) DSSD3, and (c) DSSD1.  $\theta_{pp}$  is the opening angle between  $p_1$  and  $p_2$  in which three pixels were fired simultaneously.

measurement, the average intensity and purity of  $^{27}\text{S}$  delivered to the detection array (shown in Fig. 1) were 0.14 pps and 0.024%, respectively. Under a continuous-beam mode, the isotopes of interest were implanted into three W1-type double-sided silicon strip detectors (DSSDs) with thicknesses of 142  $\mu\text{m}$  (DSSD1), 40  $\mu\text{m}$  (DSSD2), and 304  $\mu\text{m}$  (DSSD3) in a certain proportion. Each DSSD was segmented into 16 horizontal and 16 vertical strips with an active area of  $5 \times 5 \text{ cm}^2$ , providing a pixel resolution of  $3.1 \times 3.1 \text{ mm}^2$  for the position measurement for charged particles. The thinnest DSSD2 installed between DSSD1 and DSSD3 was mainly used to detect low-energy protons to reduce the peak shifts from the  $\beta$ -summing effect [19,20]. The thicker ones, DSSD1 and DSSD3, were employed for the measurement of high-energy protons and  $\beta$  particles. A total of  $3 \times 256$  pixels were used to encode the position and energy information of charged particles. All charged signals processed by the DSSDs were split and fed to high-gain and low-gain preamplifiers for decay charged-particles ( $\beta$  and protons) and implanted heavy-ions, respectively. The energy calibrations for all DSSDs were done by using  $\beta$ -delayed proton peaks from  $^{25}\text{Si}$  decay with known energies, which is the same as Ref. [15]. The efficiency for two-proton emission in the  $\beta$  decay of  $^{27}\text{S}$  was deduced from the efficiency curve fixed by the known  $\beta$ -delayed two-proton peaks of  $^{22}\text{Al}$  [21] and  $^{26}\text{P}$  [22], assuming a uniform efficiency of the DSSDs for two-proton emission from  $^{22}\text{Al}$ ,  $^{26}\text{P}$ , and  $^{27}\text{S}$  decays [15]. A 1546- $\mu\text{m}$ -thick quadrant silicon detector (QSD1) was placed behind DSSD3 for  $\beta$  particle measurements. In addition, another two quadrant silicon detectors (QSD2, QSD3) with a similar thickness of 300  $\mu\text{m}$  were installed at the end of the silicon array to serve as veto detectors to reduce light-particle contamination in the secondary beam.  $\gamma$  rays were detected by five Clover-type high-purity Germa-

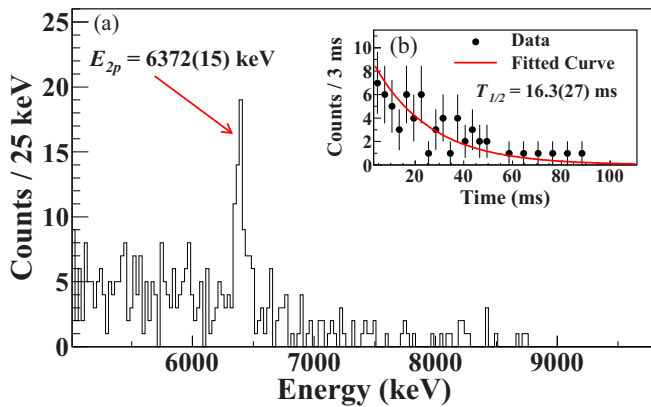


FIG. 2. (a) Energy spectrum of  $\beta$ -delayed proton from the decay of  $^{27}\text{S}$  measured by DSSD3 above 5000 keV. (b) The decay time spectrum gated on the 6372-keV peak.

nium (HPGe) detectors surrounding the silicon array. Details on the detection array and implantation-decay correlations are described in Refs. [15,23]. Al degraders with a total thickness of  $320\ \mu\text{m}$  sufficient to stop most of the  $^{27}\text{S}$  ions in the DSSD array, 40.7% in DSSD2, and 58.7% in DSSD3, respectively, were placed upstream [15].

Figure 2(a) shows the  $\beta$ -delayed proton spectrum measured by DSSD3 within a time window of ten half-lives of  $^{27}\text{S}$  after implantation. To improve the energy resolution, the  $\beta$ -summing effect on DSSD3 was suppressed by considering the anticoincidence with  $\beta$ -like particle signals in QSD1. The proton peaks with energies lower than 5 MeV have been analyzed and discussed in Ref. [15]. The 6372-keV peak corresponding to the transition from the IAS of  $^{27}\text{P}$  to the ground state of  $^{25}\text{Al}$  [12,13] was identified as a two-proton emission according to the relationship among the energy losses, positions, and path lengths of the escaping particles in different DSSDs [6]. Its half-life was obtained by fitting the time-profile illustrated in Fig. 2(b) using an exponential function plus a flat background. The fitted result of 16.3(27)ms is consistent with the  $\beta$ -decay half-life of  $^{27}\text{S}$  16.3(2) ms [15], implying that the 6372-keV peak is from the  $\beta$  decay of  $^{27}\text{S}$ . Considering the two-proton detection efficiency, the branching ratio of 2.4(5)% for the 6372-keV peak was obtained, which is consistent with Borrel's measurement [12]. However, the other two-proton transition at 5315 keV [13] was not observed in this experiment. In addition, we did not observe the 945-keV peak reported earlier [15] in our  $\gamma$  spectrum, indicating that no transition feeds the first  $3/2^+$  state of  $^{25}\text{Al}$ .

High statistics of  $^{27}\text{S}$  enabled detection of sufficient amount of proton-proton coincidences which can be attributed to the two-proton emission. The proton-proton coincidence was deduced based on the setup of the silicon array in which the DSSD2 served as a heavy ion stopper, while DSSD1 and DSSD3 were used to measure the two escaping protons. Because of its thickness of only  $40\ \mu\text{m}$ ,  $\beta$ -delayed protons could easily escape from DSSD2. When the escaping two protons ( $p_1$  and  $p_2$  in Fig. 1) were detected by the adjacent DSSD1 and/or DSSD3, three pixel would be fired simultaneously and the corresponding energies and positions would be recorded.

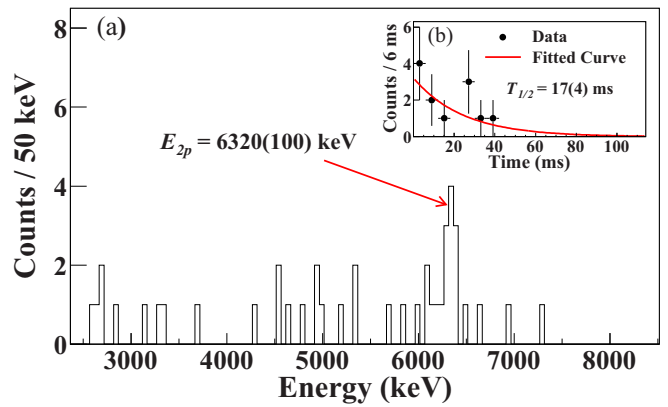


FIG. 3. (a) Summed energy spectrum of the events in which three pixels were fired using proton-proton coincident method. (b) Decay time spectrum gated on the summed energy at 6320 keV ranging from 6200 to 6500 keV.

The total decay energy of the two-proton emission should be the sum of the valid energy signals from the three fired pixels. To reduce the misidentification between the  $\beta$  particles and low-energy protons, an energy threshold of 300 keV was set for DSSD1 and DSSD3 since the energy loss for  $\beta$  particles is usually smaller than 300 keV. As a result, a total of 42 proton-proton coincident events were identified. The energy peak at 6320(100) keV shown in Fig. 3 with 12 valid events ranging from 6200 to 6500 keV, which is consistent with the 6372-keV two-proton peak, corresponds to the two-proton transition from the IAS of  $^{27}\text{P}$  to the ground state of  $^{25}\text{Al}$ . This result was confirmed by its determined half-life of 17(4) ms, as shown in Fig. 3(b). Energy-energy correlations of individual protons from  $\beta 2p$  of  $^{27}\text{S}$  were reconstructed based on path lengths, energy losses, and positions in DSSDs [15], as illustrated in Fig. 4. The red circles stand for the identified 6320-keV  $2p$  events in this experiment. The distribution of

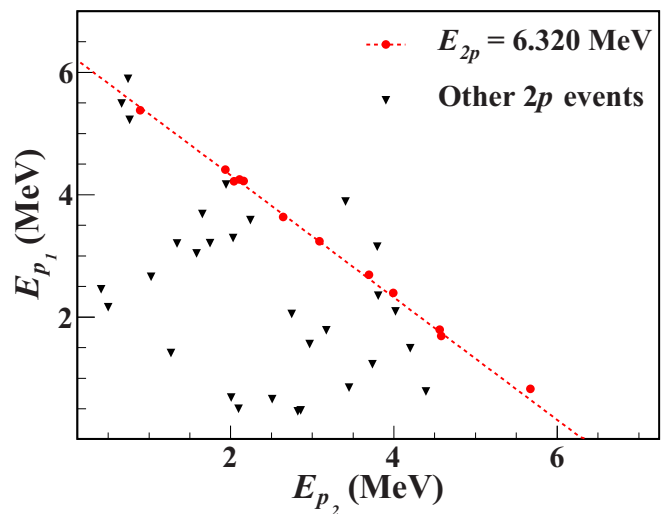


FIG. 4. Energy-energy correlations of individual protons of  $\beta 2p$  of  $^{27}\text{S}$ . The red circles and the black triangles represent the 6.320-MeV  $2p$  events and other  $2p$  events, respectively.

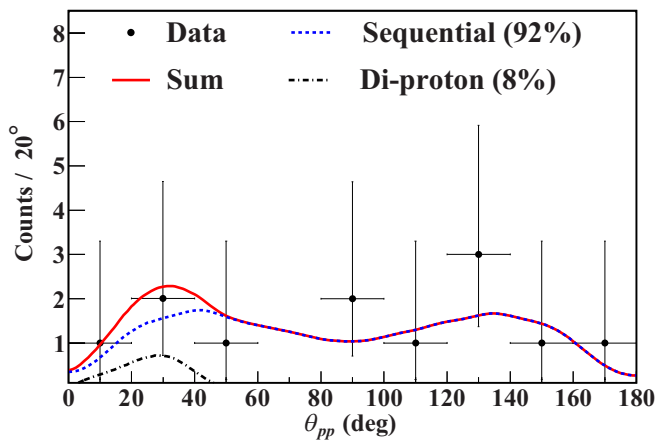


FIG. 5. Distribution of the opening angle of two protons with total energies ranging from 6200 to 6500 keV in Fig. 3. The colored lines are Monte Carlo simulation results and the black dots are the experimental results in present work.

these events seems to be uniform along the dotted line. The remaining coincident events shown with black triangles were considered other two-proton emission branches that cannot be deduced owing to low statistics.

Proton-proton angular correlations were extracted from the positions of the escaping two protons based on the proton-proton coincidence measurement method. To balance the angular resolution and angular coverage of the DSSD array, the distance between the DSSDs was set to 19 mm, resulting in a solid angle coverage of about 4.5 sr as shown in Fig. 1. The simulated angular resolution of about  $10^\circ$  was obtained based on the present DSSD array geometry. Gating on the summed energy spectrum at 6320(100) keV in Fig. 3, the measured proton-proton angular distribution is presented with black dots in Fig. 5. The spectrum shows a nearly isotropic distribution for the  $\theta_{pp}$ .

The theoretical models of the two-proton emission were well discussed in detail by Grigorenko *et al.* [24–28] and successfully applied to  $2p$  decays of many nuclear systems, such the ground state of  $^{45}\text{Fe}$  [29]. In this work, we performed Monte Carlo simulations based on a schematic model [30–33], considering two extreme cases: the diproton emission and the sequential emission, to better understand experimental angular correlations, and to investigate the mechanisms of the  $\beta 2p$  of  $^{27}\text{S}$ . The diproton emission assumes that a preformed  $^2\text{He}$  resonance with the quasibound  $^1S_0$  configuration in the parent nucleus penetrates the Coulomb barrier and breaks up into two protons outside the barrier [30], whereas the sequential emission is a two-stage procedure, in which two protons are sequentially emitted with

an intermediate state involved. The DSSD array geometry, energy resolution, energy detection threshold, and experimental heavy ion implantation distributions were taken into account in the simulations. The simulations indicated that the diproton and sequential emissions show different trends. The angular distribution of the diproton emission tends to have a marked peak at around  $30^\circ$  due to a quasibound  $s$ -singlet configuration as shown by the black dot-dashed line in Fig. 5. On the other hand, the simulated angular distribution of the sequential emission is approximately isotropic. The observed “double hump” is caused by geometrical effects due to detector arrangements. Since the three DSSDs were placed parallel to each other, the detection efficiency of two protons with an opening angle around  $90^\circ$  was relatively small, resulting in a much reduced effective angular distribution shown by the blue dashed line in Fig. 5. By fitting the experimental data with the Monte Carlo simulation results using the maximum-likelihood method, sequential emission with branching ratio of  $92_{-16}^{+8}\%$  was observed as shown in Fig. 5. This result indicates that the dominant mechanism for the  $2p$  emission from the IAS of  $^{27}\text{P}$  to the ground state of  $^{25}\text{Al}$  is of sequential nature.

In summary, the  $\beta 2p$  of  $^{27}\text{S}$  was studied. The experiment was carried out with a silicon array consisted of three DSSDs with different thicknesses using RIBLL1 at HIRFL, Lanzhou. A two-proton emission from the IAS of  $^{27}\text{P}$  to the ground state of  $^{25}\text{Al}$  was observed at 6372(15) keV with a branching ratio of 2.4(5)% in the  $\beta$  decay of  $^{27}\text{S}$ . The angular distribution for this two-proton branch was also measured to study the two-proton emission mechanism. Comparing with the simulation results, it was found that the dominant component for the two-proton emission in the  $^{27}\text{S}$   $\beta$  decay is the sequential emission. A small contribution of diproton component cannot be considered the evidence for strong angular correlations due to insufficient statistics. Further experiments with higher statistics and detailed theoretical discussion are needed.

We wish to acknowledge the support of the HIRFL operations staff for providing high-quality beams. This work is supported by the Strategic Priority Research Program of the Chinese Academy of Sciences, Grant No. XDB34010300, the Ministry of Science and Technology of China under National Key R&D Programs No. 2018YFA0404404 and No. 2016YFA0400503 and National Natural Science Foundation of China under Grants No. U1932206, No. U1632136, No. 11635015, No. 11805120, No. 11705244, No. U1432246, No. 11775316, No. 11775277, No. U1732145, No. 11705285, No. U1867212, No. 11805280, No. 11825504, No. 11675229, and No. 11490562, and by the Continuous Basic Scientific Research Project No. WDJC-2019-13.

[1] B. Blank and M. Płoszajczak, Two-proton radioactivity, *Rep. Prog. Phys.* **71**, 046301 (2008).

[2] B. Blank and M. J. G. Borge, Nuclear structure at the proton drip line: Advances with nuclear decay studies, *Prog. Part. Nucl. Phys.* **60**, 403 (2008).

- [3] M. Pfützner, M. Karny, L. V. Grigorenko, and K. Riisager, Radioactive decays at limits of nuclear stability, *Rev. Mod. Phys.* **84**, 567 (2012).
- [4] V. I. Goldanskii, Emission of  $\beta^+$ -delayed pairs of protons and doubly  $\beta^+$ -delayed protons and  $\alpha$  particles, *JETP Lett.* **32**, 554 (1980).
- [5] M. D. Cable, J. Honkanen, R. F. Parry, S. H. Zhou, Z. Y. Zhou, and J. Cerny, Discovery of Beta-Delayed Two-Proton Radioactivity:  $^{22}\text{Al}$ , *Phys. Rev. Lett.* **50**, 404 (1983).
- [6] X. X. Xu, C. J. Lin, L. J. Sun, J. S. Wang, Y. H. Lam, J. Lee, D. Q. Fang, Z. H. Li, N. A. Smirnova, C. X. Yuan, L. Yang, Y. T. Wang, J. Li, N. R. Ma, K. Wang, H. L. Zang, H. W. Wang, C. Li, M. L. Liu, J. G. Wang *et al.*, Observation of  $\beta$ -delayed two-proton emission in the decay of  $^{22}\text{Si}$ , *Phys. Lett. B* **766**, 312 (2017).
- [7] M. J. G. Borge, Beta-delayed particle emission, *Phys. Scr.* **152**, 014013 (2013).
- [8] B. Alex Brown, Isospin-Forbidden  $\beta$ -Delayed Proton Emission, *Phys. Rev. Lett.* **65**, 2753 (1990).
- [9] Y. T. Wang, D. Q. Fang, K. Wang, X. X. Xu, L. J. Sun, P. F. Bao, Z. Bai, X. G. Cao, Z. T. Dai, B. Ding, W. B. He, M. R. Huang, S. L. Jin, C. J. Lin, M. Lv, L. X. Liu, Y. Li, P. Ma, J. B. Ma, J. S. Wang *et al.*, Observation of  $\beta$ -delayed  $^2\text{He}$  emission from the proton-rich nucleus  $^{22}\text{Al}$ , *Phys. Lett. B* **784**, 12 (2018).
- [10] H. O. U. Fynbo, M. J. G. Borge, L. Axelsson, J. Äystö, U. C. Bergmann, L. M. Fraile, A. Honkanen, P. Hornshøj, Y. Jading, A. Jokinen, B. Jonson, I. Martel, I. Mukha, T. Nilsson, G. Nyman, M. Oinonen, I. Piqueras, K. Riisager, T. Siiskonen, M. H. Smedberg, O. Tengblad *et al.*, The  $\beta 2p$  decay mechanism of  $^{31}\text{Ar}$ , *Nucl. Phys. A* **677**, 38 (2000).
- [11] I. Matea, N. Adimi, B. Blank, G. Canchel, J. Giovinazzo, M. J. G. Borge, R. Domínguez-Reyes, O. Tengblad, and J.-C. Thomas, The silicon cube detector, *Nucl. Instrum. Methods Phys. Res., Sect. A* **607**, 576 (2009).
- [12] V. Borrel, J. C. Jacmart, F. Pougheon, R. Anne, C. Detraz, D. Guillemaud-Mueller, A. C. Mueller, D. Bazin, R. Del Moral, J. P. Dufour, F. Hubert, M. S. Pravikoff, and E. Roeckl,  $^{31}\text{Ar}$  and  $^{27}\text{S}$ : Beta-delayed two-proton emission and mass excess, *Nucl. Phys. A* **531**, 353 (1991).
- [13] G. Canchel, L. Achouri, J. Äystö, R. Béraud, B. Blank, E. Chabanat, S. Czajkowski, P. Dendooven, A. Emsallem, J. Giovinazzo, J. Honkanen, A. Jokinen, M. Lewitowicz, C. Longour, F. de Oliveira Santos, K. Peräjärvi, M. Staniou, and J. C. Thomas, The  $\beta$ -delayed one- and two-proton emission of  $^{27}\text{S}$ , *Eur. Phys. J. A* **12**, 377 (2001).
- [14] L. Janiak, N. Sokolowska, A. A. Bezbakh, A. A. Ciemny, H. Czyrkowski, R. Dabrowski, W. Dominik, A. S. Fomichev, M. S. Golovkov, A. V. Gorshkov, Z. Janas, G. Kamiński, A. G. Knyazev, S. A. Krupko, M. Kuich, C. Mazzocchi, M. Mentel, M. Pfützner, P. Pluciński, M. Pomorski *et al.*,  $\beta$ -delayed proton emission from  $^{26}\text{P}$  and  $^{27}\text{S}$ , *Phys. Rev. C* **95**, 034315 (2017).
- [15] L. J. Sun, X. X. Xu, C. J. Lin, J. Lee, S. Q. Hou, C. X. Yuan, Z. H. Li, J. José, J. J. He, J. S. Wang, D. X. Wang, H. Y. Wu, P. F. Liang, Y. Y. Yang, Y. H. Lam, P. Ma, F. F. Duan, Z. H. Gao, Q. Hu, Z. Bai *et al.*,  $\beta$ -decay spectroscopy of  $^{27}\text{S}$ , *Phys. Rev. C* **99**, 064312 (2019).
- [16] L. J. Sun, X. X. Xu, S. Q. Hou, C. J. Lin, J. José, J. Lee, J. J. He, Z. H. Li, J. S. Wang, C. X. Yuan, F. Herwig, J. Keegans, T. Budner, D. X. Wang, H. Y. Wu, P. F. Liang, Y. Y. Yang, Y. H. Lam, P. Ma, F. F. Duan *et al.*, Experimentally well-constrained masses of  $^{27}\text{P}$  and  $^{27}\text{S}$ : Implications for studies of explosive binary systems, *Phys. Lett. B* **802**, 135213 (2020).
- [17] W. L. Zhan, J. W. Xia, H. W. Zhao, G. Q. Xiao, Y. J. Yuan, H. S. Xu, K. D. Man, P. Yuan, D. Q. Gao, X. T. Yang, M. T. Song, X. H. Cai, X. D. Yang, Z. Y. Sun, W. X. Huang, Z. G. Gan, and B. W. Wei, HIRFL today, *Nucl. Phys. A* **805**, 533c (2008).
- [18] Z. Sun, W.-L. Zhan, Z.-Y. Guo, G. Xiao, and J.-X. Li, RIBLL, the radioactive ion beam line in Lanzhou, *Nucl. Instrum. Methods Phys. Res., Sect. A* **503**, 496 (2003).
- [19] J. Görres, M. Wiescher, K. Scheller, D. J. Morrissey, B. M. Sherrill, D. Bazin, and J. A. Winger,  $\beta$ -delayed proton decay of  $^{20}\text{Mg}$  and its astrophysical implications, *Phys. Rev. C* **46**, R833 (1992).
- [20] W. Trinder, E. G. Adelberger, B. A. Brown, Z. Janas, H. Keller, K. Krumbholz, V. Kunze, P. Magnus, F. Meissner, A. Piechaczek, M. Pfützner, E. Roeckl, K. Rykaczewski, W.-D. Schmidt-Ott, and M. Weber, Study of the  $\beta$  decays of  $^{37}\text{Ca}$  and  $^{36}\text{Ca}$ , *Nucl. Phys. A* **620**, 191 (1997).
- [21] N. L. Achouri, F. de Oliveira Santos, M. Lewitowicz, B. Blank, J. Äystö, G. Canchel, S. Czajkowski, P. Dendooven, A. Emsallem, J. Giovinazzo, N. Guillet, A. Jokinen, A. M. Laird, C. Longour, K. Peräjärvi, N. Smirnova, M. Staniou, and J. C. Thomas, The  $\beta$ -decay of  $^{22}\text{Al}$ , *Eur. Phys. J. A* **27**, 287 (2006).
- [22] J.-C. Thomas, L. Achouri, J. Äystö, R. Béraud, B. Blank, G. Canchel, S. Czajkowski, P. Dendooven, A. Emsallem, J. Giovinazzo, N. Guillet, J. Honkanen, A. Jokinen, A. Laird, M. Lewitowicz, C. Longour, F. de Oliveira Santos, K. Peräjärvi, and M. Staniou, Beta-decay properties of  $^{25}\text{Si}$  and  $^{26}\text{P}$ , *Eur. Phys. J. A* **21**, 419 (2004).
- [23] L. J. Sun, X. X. Xu, C. J. Lin, J. S. Wang, D. Q. Fang, Z. H. Li, Y. T. Wang, J. Li, L. Yang, N. R. Ma, K. Wang, H. L. Zang, H. W. Wang, C. Li, C. Z. Shi, M. W. Nie, X. F. Li, H. Li, J. B. Ma, P. Ma *et al.*, A detection system for charged-particle decay studies with a continuous-implantation method, *Nucl. Instrum. Methods Phys. Res., Sect. A* **804**, 1 (2015).
- [24] L. V. Grigorenko, R. C. Johnson, I. G. Mukha, I. J. Thompson, and M. V. Zhukov, Two-proton radioactivity and three-body decay: General problems and theoretical approach, *Phys. Rev. C* **64**, 054002 (2001).
- [25] L. V. Grigorenko and M. V. Zhukov, Two-proton radioactivity and three-body decay. II. Exploratory studies of lifetimes and correlations, *Phys. Rev. C* **68**, 054005 (2003).
- [26] L. V. Grigorenko and M. V. Zhukov, Two-proton radioactivity and three-body decay. III. Integral formulas for decay widths in a simplified semianalytical approach, *Phys. Rev. C* **76**, 014008 (2007).
- [27] L. V. Grigorenko and M. V. Zhukov, Two-proton radioactivity and three-body decay. iv. connection to quasiclassical formulation, *Phys. Rev. C* **76**, 014009 (2007).
- [28] L. V. Grigorenko, I. A. Egorova, M. V. Zhukov, R. J. Charity, and K. Miernik, Two-proton radioactivity and three-body decay. V. Improved momentum distributions, *Phys. Rev. C* **82**, 014615 (2010).
- [29] K. Miernik, W. Dominik, Z. Janas, M. Pfützner, L. Grigorenko, C. R. Bingham, H. Czyrkowski, M. Ćwiok, I. G. Darby, R. Dabrowski, T. Ginter, R. Grzywacz, M. Karny, A. Korgul, W. Kuśmierz, S. N. Liddick, M. Rajabali, K. Rykaczewski, and A. Stolz, Two-Proton Correlations in the Decay of  $^{45}\text{Fe}$ , *Phys. Rev. Lett.* **99**, 192501 (2007).

- [30] S. E. Koonin, Proton pictures of high-energy nuclear collisions, *Phys. Lett. B* **70**, 43 (1977).
- [31] C. J. Lin, X. X. Xu, H. M. Jia, F. Yang, F. Jia, S. T. Zhang, Z. H. Liu, H. Q. Zhang, H. S. Xu, Z. Y. Sun, J. S. Wang, Z. G. Hu, M. Wang, R. F. Chen, X. Y. Zhang, C. Li, X. G. Lei, Z. G. Xu, G. Q. Xiao, and W. L. Zhan, Experimental study of two-proton correlated emission from  $^{29}\text{S}$  excited states, *Phys. Rev. C* **80**, 014310 (2009).
- [32] X. X. Xu, C. J. Lin, H. M. Jia, F. Yang, F. Jia, Z. D. Wu, S. T. Zhang, Z. H. Liu, H. Q. Zhang, H. S. Xu, Z. Y. Sun, J. S. Wang, Z. G. Hu, M. Wang, R. F. Chen, X. Y. Zhang, C. Li, X. G. Lei, Z. G. Xu, G. Q. Xiao, and W. L. Zhan, Investigation of two-proton emission from excited states of the odd- $z$  nucleus  $^{28}\text{P}$  by complete-kinematics measurements, *Phys. Rev. C* **81**, 054317 (2010).
- [33] X. X. Xu, C. J. Lin, H. M. Jia, F. Yang, H. Q. Zhang, Z. H. Liu, Z. D. Wu, L. Yang, P. F. Bao, L. J. Sun, H. S. Xu, J. S. Wang, Y. Y. Yang, Z. Y. Sun, Z. G. Hu, M. Wang, S. L. Jin, J. L. Han, N. T. Zhang, S. Z. Chen *et al.*, Correlations of two protons emitted from excited states of  $^{28}\text{S}$  and  $^{27}\text{P}$ , *Phys. Lett. B* **727**, 126 (2013).